AUTHOR(S): NWOGU, N., OKON, E. and GOBINA, E.

TITLE: Integration of gas transport through a composite catalytic inorganic ceramic membrane for environmental gas separation processes.

YEAR: 2014

Publisher citation: NWOGU, N., OKON, E. and GOBINA, E. 2014. Integration of gas transport through a composite catalytic inorganic ceramic membrane for environmental gas separation processes. International journal of scientific engineering and technology [online], 3(9), pages 1184-1188. Available from: http://www.ijset.com/ijset/publication/v3s9/IJSET_2014_914.pdf

OpenAIR citation: NWOGU, N., OKON, E. and GOBINA, E. 2014. Integration of gas transport through a composite catalytic inorganic ceramic membrane for environmental gas separation processes. International journal of scientific engineering and technology, 3(9), pages 1184-1188. Held on OpenAIR [online]. Available from: https://openair.rgu.ac.uk

Integration of Gas Transport through a Composite Catalytic Inorganic Ceramic Membrane for Environmental Gas Separation Processes

Ngozi Nwogu, Edidiong Okon,Edward Gobina
Center for Process Integration and Membrane Technology (CPIMT), School of Engineering. The Robert Gordon University Aberdeen, AB10 7GJ, United Kingdom.
E-mail: *Corresponding Author: e.gobina@rgu.ac.uk

Abstract :***This work presents the transport behaviour of carrier gases with inorganic ceramic membrane used for environmental gas separations at 289K and 0.01-1 bar. The gases tested include: Helium (He), Nitrogen (N_2) Carbon dioxide (CO_2) and Argon (Ar). The Knudsen ideal selectivity ratio of 0.95, 0.3 and 0.79 for Ar/CO_2, He/CO_2 and N_2/CO_2 gas respectively was slightly higher than the theoretical selectivity of the gases. The gas permeance was found to decrease with increase in gauge pressure indicating mass transfer limitations. However, at a relatively low pressure of 0.1 bar, Knudsen diffusion mechanism was dominant for He and N_2 gases flow across the modified ceramic membrane in relation to the inverse proportionality of the square root of their molecular weights. Scanning electron microscopy (SEM) was used to determine the pore size distribution of the α-Al_2O_3 ceramic support.***

Keywords: Permeance, Selectivity, Knudsen diffusion and Inorganic ceramic membrane.

I Introduction

Power generation accounts for approximately one third of the total carbon dioxide (CO_2) emissions globally. CO_2 free gas-powered plants are based on carbon dioxide being selectively removed from the waste flue gases and deposited in the ground or in enhanced oil recovery applications. However, before CO_2 can be utilized, it must be separated from the waste flue gases. The current methods used for this type of separation are not easily affordable since they require the use of chemical adsorbents. Polymeric membranes are not very stable under flue gas conditions. Inorganic membranes are going to make a total transformation in the entire system [1]. Membrane-based technology in the past years has been used extensively in several applications including pharmaceuticals, biochemical engineering, water treatment and food industry [2]. Ceramic membranes such as zeolite or silica membranes are generally suitable for applications which employ high temperature and corrosive or organic media [3]. In carrying out esterification by reactive separations for example, ceramic membrane has been seriously considered in the membrane process since this membrane can selectively eliminate water as a product by shifting the equilibrium in esterification reaction and can also withstand the effect of high temperatures. Materials such as Al_2O_3 (alumina), TiO_2 (titania), ZrO_2 (zirconia) and SiO_2 (silica) or a combination of these are the most common materials used for ceramic membranes [8]. Ceramic membrane can exist either as a microporous thin film or a mesoporous or a combination of these. The two major processes that play a significant role in the gas transport is the diffusion and sorption mechanism. Diffusion explains the rate at which gas molecule moves across the membrane whereas sorption describe the interaction between the surface of the membrane and the gas molecule [4]. Based on the operating conditions such as temperature and pressure, the nature of the membrane including pore size distribution and the permeating molecule; the gas permeation behaviour through an inorganic ceramic membrane can be explained using different transport mechanisms including viscous flow, Knudsen diffusion, molecular sieving, capillary condensation and surface diffusion respectively. In Knudsen mechanism of transport, collision occurs between the gas molecule and the membrane pore walls. Viscous flow occurs at higher temperature if the pore radius of the membrane is larger than the mean free path of the permeating gas molecule [5]. Composite membrane can be obtained by coating a porous support through immersion in a colloidal solution called sol gel. The different coating methods include: slip coating or spin coating and dip-coating [6].

II Experimental

The gas transport through a porous inorganic ceramic membrane was performed using single gases including nitrogen (N_2) Argon (Ar) carbon dioxide (CO_2) helium (He), at room temperature (298 K) and different gauge pressure of 0.01-1(Bar). The membrane pore size was 15 nm. The flow meter (L/min) was used to determine the gas flow rate. The inner and outer radius of the membrane was 7 mm and 10 mm respectively, whereas the total length of the membrane was measured to be 36.6 cm. Figure 1 shows the schematic diagram of the membrane dip-coating process.

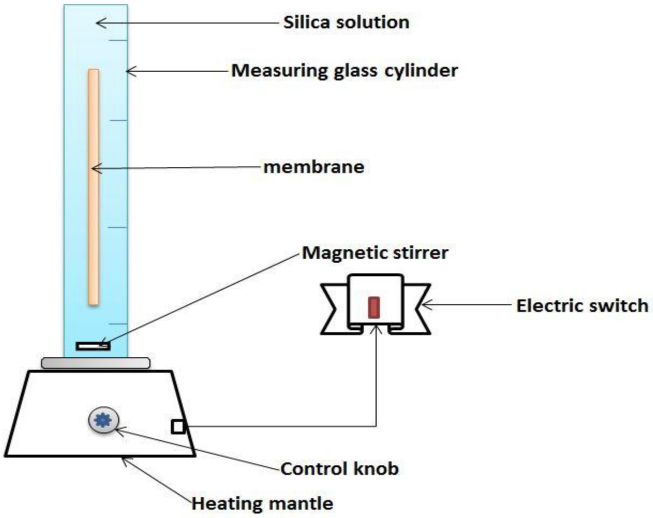

Figure 1: Schematic diagram of membrane preparation setup

The membrane was weighed to determine the actual measurement before and after modification. The membrane thickness was calculated using the formula [11]:

$$L = \frac{W2 - W1}{A\rho(1-\varepsilon)} \qquad (1)$$

Where L = Membrane thickness (m), W_2 = total weight of the support and membrane (g), W_1 = weight of the alumina support (g), A= membrane area (m), ρ = theoretical density of alumina (kgm^3) and ε = porosity of the membrane (%).

The membrane modification was carried out as thus: A certain amount of isobutene was measured into a 1000 mL glass cylinder and a known amount of silicon elastomer was added to the solution together with a known amount of sylgard. The mixture was allowed to stir for 30 min. After 30 min, the membrane was dipped into the solution and allowed in the solution for 30 min. After 30 min, the support was taken out from the solution and dried for 30 min in the atmosphere. The support was then transferred into the oven and allowed in the oven for 2 hrs at a constant temperature of 65 ^{o}C [9]. Figure 2 shows a schematic setup of gas permeation test. It consists of gas delivery system, pressure delivery system, permeate gauge pressure, valve, membrane, reactor, retentate gauge pressure and flow meter.

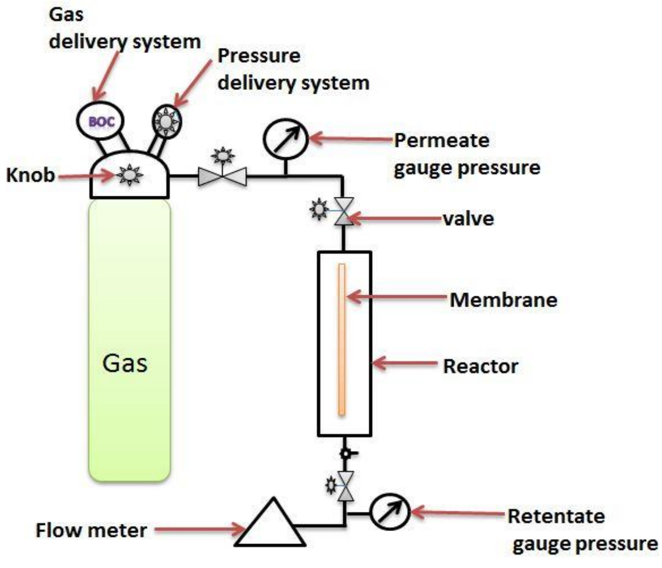

Figure 2; Gas permeation setup.

III Result and Discussion

Scanning electron microscopy was used to further investigate the pore size distribution of the ceramic support. The results obtained in Figure 3a and b showed that the pore size of the inner surface was found to be smaller with scale of 2 µm than the outer surface with the scale of 10 µm. The larger pore size observed in the outer surface image was assumed to originate as the result of the effect of the interaction between the silica solution that was used in coating the membrane surface. The surfaces of the dip-coated membrane were observed to be uniform without any noticeable crack on the surface indicating defect-free membrane [5].

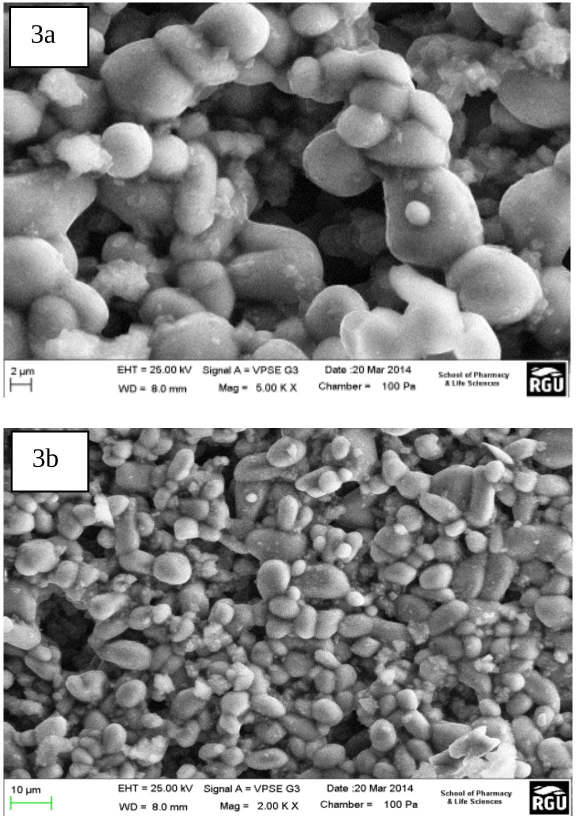

Figure 3a and b: (a) SEM image of the inner surface and (b) SEM image of the outer surface of α-ceramic membrane

The permeance of each gas was calculated using the equation:

$$Q_i = \frac{F_i}{A \text{ x } t \text{ x } \Delta P} \qquad (2)$$

Where Q_i = gas permeance (mol m^{-2} s^{-1} Pa^{-1}), F_i = gas flow rate (l/min), *A*= membrane surface area (m^2), t = unit time (s) and ΔP = pressure difference (bar). Figure 4 and 5 shows the effect of the pressure on the permeance of the different gases.

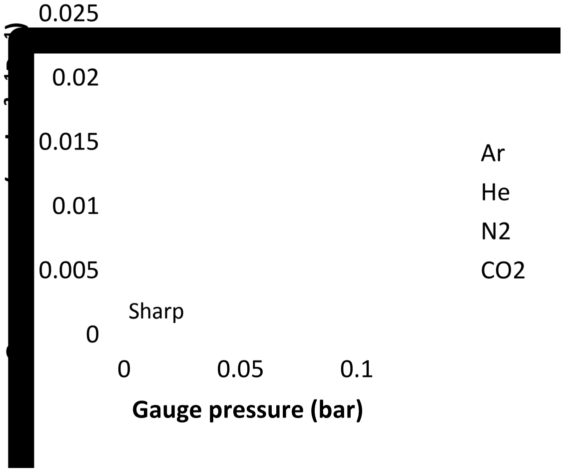

Figure 4: Gas permeance (molm^{-2}s^{-1} Pa^{-1}) against gauge pressure between 0.01 and 0.09 (bar).

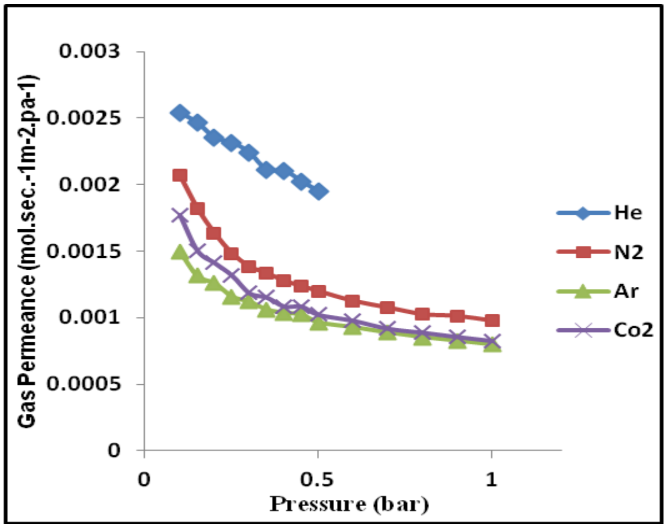

Figure 5: Gas permeance (molm^{-2}s^{-1} Pa^{-1}) against gauge pressure between 0.1 and 1.0 (bar).

It can be seen from Figure 4 that the gas permeance decreased with increase in gauge pressure. The sharp decrease between 0 and 0.02 bar could be an indication of mass transfer limitation between the gas phase and the membrane surface. This limitation could be eliminated by increasing the annular space in the permeator. However it was observed that the sharp decrease diminished with an increase in pressure as shown in Figure 5. In addition the Knudsen flow mechanism was more prevalent with an increase in the pressure drop. This result corroborates with a similar study by Li et al. [10], on the experimental and modelling study of gas transport through a composite ceramic membrane which consist of α-Al_2O_3 support. In their study, the gas permeance was found to decrease with increase in gauge pressure indicating limitation due to mass transfer of gas transport through the ceramic membrane.

The relationship between gas permeance and the inverse of square root of their molecular weight was investigated to determine the various flow mechanisms that were applicable. In Figure 6, the plot of gas permeance against the inverse of square root of their molecular weights at a pressure of 0.1 shows that for CO_2, Ar and N_2 gases, Knudsen flow mechanism was dominant. He gas with a lower molecular weight of 4 had a higher permeance followed by N_2. CO_2 with the highest molecular weight of 44 permeated faster than Ar. This could be as a result of the CO_2 gas molecular attraction to the membrane pore walls as the adsorbing gas. An increase in the pressure to 0.5bar in Figure 7 gives an indication of a slight deviation in the flow mechanism existing between CO_2 and Ar gases. Their permeance rates were quite close and a possibility that at a higher pressure, Ar gas permeance might exceed that of CO_2 as expected of Knudsen flow diffusion mechanism.

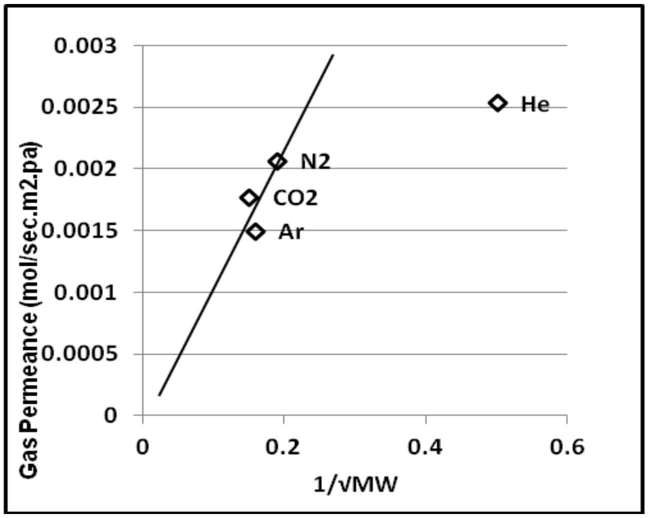

Figure 6: Gas permeance (molm^{-2}s^{-1} Pa^{-1}) against inverse of square root of gas molecular weight at 0.1 bar.

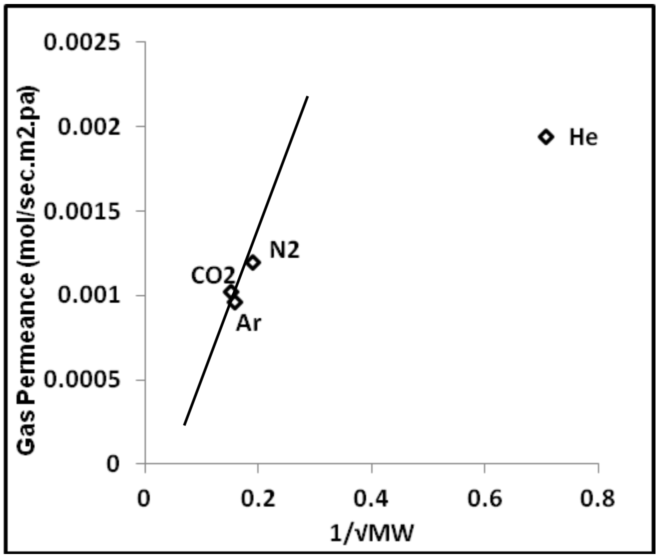

Figure 7: Gas permeance (molm^{-2}s^{-1} Pa^{-1}) against inverse of square root of gas molecular weight at 0.5 bar.

Figure 8 shows more results obtained with gas permeance in relation to the kinetic diameter of the He, N_2, CO_2 and Ar. As shown, the gas permeance is not in a precise order of their kinetic diameter. He with the lowest kinetic diameter (2.65Å) permeated faster than the other gases. However, N_2 gas with the highest kinetic diameter (3.64Å) has higher permeation in comparison to CO_2 (3.3 Å) and Ar (3.4Å). The flow mechanism present cannot be suggested to be molecular sieving type of diffusion but for the case for He gas.

The order of gas permeance, molecular weight and the kinetic diameter of the gases used is as followed:

Order of molecular weight:
CO_2 (44) > Ar (40) > N_2 (28) > He (4).

Order of gas permeance:
He > N_2 > CO_2 > Ar

Order of gas kinetic diameter:
N_2 (3.64Å) > Ar (3.4Å) > CO_2 (3.3 Å) > He (2.65Å)

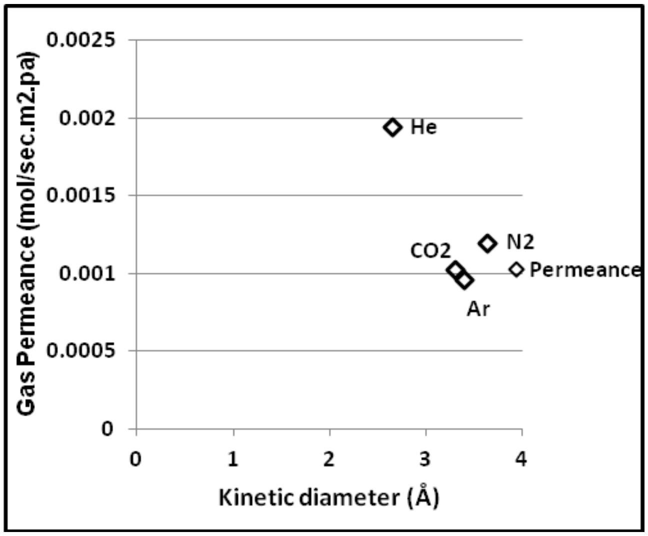

Figure 8: Gas permeance (molm^{-2}s^{-1} Pa^{-1}) as a function of kinetic diameter at 298 K and 0.5 bar

The Knudsen experimental selectivity was calculated using the permeance ratio of CO_2 with respect to each gas at each pressure gauge (bar). The data shown in Table 1 is plotted in Figure 9 below

Table 1: Permeance ratio of CO_2/Ar, CO_2/He and CO_2/N_2 gas.

Gauge pressure (bar)	Permeance ratio of CO_2/Ar	Permeance ratio of CO_2/He	Permeance ratio of CO_2/N_2
0.01	0.804	0.643	0.865
0.02	0.898	0.657	0.844
0.03	0.811	0.602	0.854
0.04	0.696	0.588	0.759
0.05	0.675	0.572	0.855
0.06	0.724	0.533	0.819
0.07	0.675	0.496	0.769
0.08	0.699	0.510	0.773
0.09	0.728	0.525	0.789

The Knudsen selectivity (α_k) was calculated as the square root of the molecular weight of either Ar, He or N_2 gas over CO_2 at each gauge pressure (bar), using the following equation:

$$\alpha_k = \sqrt{\frac{M_{wti}}{Mwt_{CO2}}} \qquad (3)$$

Where α_k = Knudsen selectivity, M_{wti} = Molecular weight of either Ar, He or N_2 (g/mol) and Mwt_{CO2} = Molecular weight of CO_2 (g/mol).

Table 2: Calculated Knudsen selectivity values for the gases.

Gases	**Knudsen selectivity (α_k)**
α_kAr/CO_2	0.95
α_kHe/CO_2	0.30
$\alpha_k$$N_2$/$CO_2$	0.79

The results obtained in Table 2, shows that Knudsen selectivity value of α_kAr/CO_2, (0.95) was slightly higher than the permeance ratio in Table 1. These suggest that there could be another mechanism of transport that was responsible for the separation of these gases. However, Knudsen selectivity value of α_kHe/CO_2 (0.30) was lower than the permeance ratio, which could suggest a good separation for He gas. Figure 9 shows a plot of the permeance ratio of CO_2 with the respective gas against gauge pressure (bar) at 298 K.

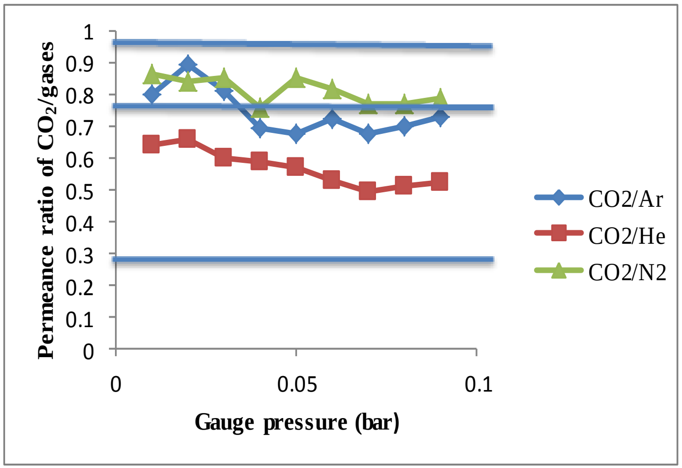

Figure 9: Permeance ratio of CO_2/Ar, CO_2/N_2 and CO_2/He against gauge pressure (bar) at 298 K.

IV Conclusion

The transport behaviour of four gases He, N_2, CO_2 and Ar with inorganic ceramic membrane was investigated. The gas permeance was found to decrease with respect to pressure between 0.01 to 0.09 bar as a result of mass transfer limitation. An increase in the pressure to 0.5 bar was observed to have a slight deviation in the flow mechanism existing for CO_2 and Ar gases with almost the same permeance rate. There is a possibility that at a much higher pressure, Ar gas permeance might exceed that of CO_2 as expected of Knudsen flow diffusion mechanism and gas molecule attraction to the membrane surface. The presence of molecular sieve mechanism was also confirmed for He. The Knudsen selectivity value of He/CO_2 was lower than the permeance ratio in contrast to other gases, which suggests a better adsorption of these gases. However, the SEM result of the inner surface showed a smaller pore in contrast to the outer surface.

NOMENCLATURE

Symbols

$MwtCO_2$ = Gas molecular weight of Mwt_{CO2} (g/mol).
Mwti = Gas molecular weight (g/mol)
Q_i = Gas flow rate (mol s^{-1})
L = Membrane thickness (m),
ΔP = Pressure drop
A = Surface area of the membrane (m^2)
T = Temperature (Kelvin)
W_2 = total weight of the support and membrane (g)
W_1 = weight of the alumina support (g),

Greek symbol

ρ = theoretical density of alumina (kgm^3)
ε = porosity of the membrane (%).

REFERENCE

i. Yave W, Car A, Peinemann K. Nanostructured membrane material designed for carbon dioxide separation. Journal of Membrane Science. 2010; 350(1–2):124-129.

ii. LIU G, WEI W, JIN W, XU N. Polymer/ceramic composite membranes and their application in pervaporation process. Chinese Journal of Chemical Engineering. 2012; 20(1):62-70.

iii. Lindqvist K, Lidén E. Preparation of alumina membranes by tape casting and dip coating. Journal of the European Ceramic Society. 1997; 17(2):359-366.

iv. Li W, Liu W, Xing W, Xu N. Esterification of Acetic Acid and n-Propanol with Vapor Permeation Using NaA Zeolite Membrane. Industrial & Engineering Chemistry Research. 2013; 52(19):6336-6342.

v. McCool BA, Hill N, DiCarlo J, DeSisto WJ. Synthesis and characterization of mesoporous silica membranes via dip-coating and hydrothermal deposition techniques. Journal of Membrane Science. 2003; 218(1–2):55-67.

vi. Lee D, Oyama ST. Gas permeation characteristics of a hydrogen selective supported silica membrane. Journal of Membrane Science. 2002; 210(2):291-306.

vii. Pandey P, Chauhan R. Membranes for gas separation. Progress in Polymer Science. 2001; 26(6):853-893.

viii. Caro J, Noack M, Kölsch P, Schäfer R. Zeolite membranes – state of their development and perspective. Microporous and Mesoporous Materials. 2000; 38(1):3-24.

ix. Gobina E. Apparatus and Method for separating gases. United state patent. Patent No.: US 7,048,778 B2. 2006. RobertGordon University, Aberdeen, UK.

x. Li, H., U. Schygulla, J. Hoffmann, P. Niehoff, K. Haas-Santo, and R. Dittmeyer. "Experimental and modeling study of gas transport through composite ceramic membranes." Chemical Engineering Science 108 (2014): 94-102.

xi. Zhu J, Fan Y, Xu N. Modified dip-coating method for preparation of pinhole-free ceramic membranes. Journal of Membrane Science. 2011; 367(1):14-20.